Article no. 10

THE CIVIL ENGINEERING JOURNAL 2-2017

DYNAMICAL RESPONSE OF AN ELASTIC SUPPORTING PILE EMBEDDED IN SATURATED SOIL UNDER HORIZONTAL VIBRATION

Shuzhen Feng [1], *Xiaotian Liu* [2], *and Hai Cui* [3]

1. *Nanjing Institute of Railway Technology, Nanjing 210031, China; 437727006@qq.com*
2. *College of Civil Engineering, Tongji University, Shanghai 200092, China; 2012liuxiaotian@tongji.edu.cn*
3. *China Railway Major Bridge (Nanjing) Bridge and Tunnel Inspect & Retrofit Co., Ltd., Nanjing 2100032, China; 1244475021@qq.com*

ABSTRACT

Using the principles of soil dynamics and structural dynamics, an analytical solution for an elastic supporting pile under horizontal vibration was formulated, based on an improved beam-on-dynamic-Winkler-foundation model and taking into consideration the change along the soil depth and the inertia phase of the fluid. The degenerated impedance on the top of the elastic supporting pile was proved to be correct. The parameters influencing the horizontal vibration characteristics of the elastic supporting pile were analysed in detail, and the influence of the elastic support on the impedance on the pile-top was discussed.

KEYWORDS

Elastic support, analytical solution, horizontal vibration, pile-soil interaction

INTRODUCTION

The mechanism of pile-soil interaction in horizontal vibration of an elastic supporting pile during action of the machine is an important issue for geotechnical workers. Numerous studies on the dynamic response of pile foundations under vibration have been conducted. Novak [1], Nogami and Novak [2], and Novak and Aboul-Ella [3] have systematically studied pile-soil interactions in single-phase soil under vibration. Fixation of the underground pile may not be completely rigid when the soil around the pile is soft and the pile is not embedded deep into bedrock or when the bedrock is soft. Novak’s plane strain model uses a series of simplified algorithms of radiation damping to calculate when the pile is horizontally vibrating in saturated soil [4–6]. Some researchers have simulated the vertical dynamic response of a pipe pile, based on Biot’s 3D poroelastic theory of porous media in saturated soil, by separating the variables and the potential function to provide an analytic solution for the impedance in a pile-tip, when the pile is embedded in saturated soil [7,8]. The results will inevitably be inaccurate if the fixation of the pile is assumed to be completely rigid. In previous studies, the supporting role of the pile-tip soil against the pile has often been simplified to rigid support, but studies on the bearing contact of the pile-tip are rare. Low-strain integrity testing has been widely used in pile foundation quality detection. In this, the tubular structure is subjected to a transient point loading, and analytical solutions are obtained [9–12].

Currently, no studies have been reported on the dynamical characteristics of an elastic supporting pile embedded in saturated soil under horizontal vibration. This paper considers the components of displacement along the depth and fluid inertia of the pile. Based on the dynamic consolidation theory proposed by Biot, the dynamic characteristics of an elastic supporting pile embedded in saturated soil under horizontal vibration are obtained. The solution has broad applicability and can meet the demand of projects.

CALCULATION MODEL

Basic assumptions

The analyses in this paper are based on the following basic assumptions. The pile is assumed to be a cylinder of radius r_0, height H, and constant cross-sectional dimensions (Figure 1). The soil around the pile is saturated and is both isotropic and homogeneous. The pile of soil is isotropic, is of uniform quality, and has a constant radius. Based on an improved beam-on-dynamic-Winkler-foundation model, the gradient varies and the inertia phase of the fluid along the depth of volume stress, and the displacement components in the soil around the pile are considered. When horizontal vibration occurs, the pile and soil are only displaced laterally and vertical displacement is negligible. The bottom support of the pile is the elastic support, only can obtain motion in horizontal direction but not relative rotation. During vibration, the pile and soil are in full contact; therefore, slip and detachment do not occur. The spring anti-horizontal displacement comprises a horizontal resistance coefficient of soil k_s and a horizontal resistance coefficient of pile-tip k_p, which means that the shear resistance of the soil and the pile-tip need to resist a unit horizontal displacement.

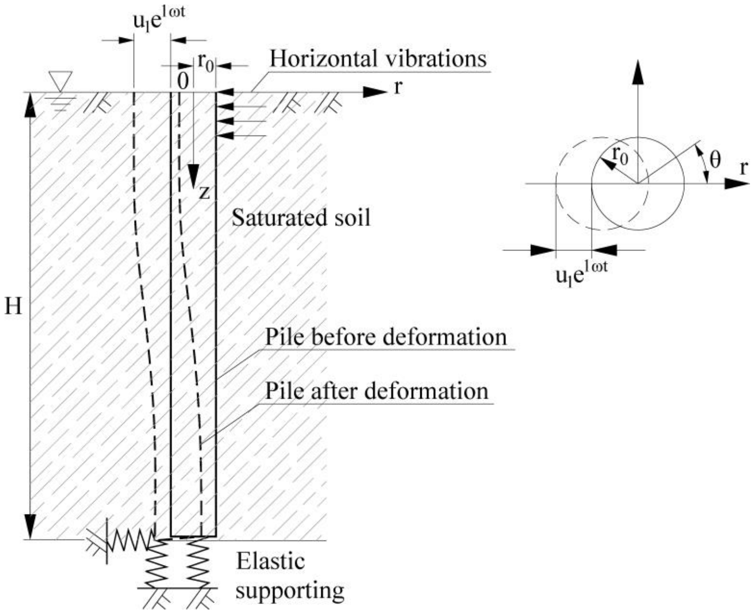

Fig. 1 - Structure diagram of an elastic supporting pile embedded in saturated soil under horizontal vibration

DOI 10.14311/CEJ.2017.02.0010

Boundary Conditions

The five boundary conditions are described below:

(1) Boundary conditions for the soil at the pile hole wall:

$$u_r(r,\theta,z,t)=u_1e^{i\omega t}\cos\theta W(z) \tag{1}$$

$$u_\theta(r,\theta,z,t)=-u_1e^{i\omega t}\sin\theta W(z) \tag{2}$$

(2) Horizontal distance continues infinitely. Displacement is attenuated to 0.

(3) Upper and lower boundary conditions for the soil:

$$\sigma_{zr}\big|_{z=0}=0,\ (\frac{\partial u_r}{\partial z}+\frac{k_s u_r}{G})\big|_{z=H}=0 \tag{3}$$

(4) Boundary conditions for the pile:

$$u'_p\big|_{z=H}=0,\ (\frac{\partial^3 u_p}{\partial z^3}+\frac{k_p}{E_pI_p}u_p)\big|_{z=H}=0 \tag{4}$$

(5) Coordination conditions of the pile and soil:

$$u_p\big|_{r=r_0}=u_r\big|_{r=r_0} \tag{5}$$

Governing Equation

According to the analysis of Zienkiewicz [13], for general soil dynamics problems, Biot's wave equation in saturated soil can be written as follows:

$$G\nabla^2u_r+(\lambda+G)\frac{\partial e}{\partial r}-\frac{G}{r^2}(2\frac{\partial u_\theta}{\partial\theta}+u_r)+G\frac{\partial^2u_r}{\partial z^2}-\alpha\frac{\partial p_f}{\partial r}=\rho\ddot{u}_r+\rho_f\ddot{w}_r \tag{6}$$

$$G\nabla^2u_\theta+(\lambda+G)\frac{1}{r}\frac{\partial e}{\partial\theta}-\frac{G}{r^2}(u_\theta-2\frac{\partial u_r}{\partial\theta})-\alpha\frac{1}{r}\frac{\partial p_f}{\partial\theta}+G\frac{\partial^2u_\theta}{\partial z^2}=\rho\ddot{u}_\theta+\rho_f\ddot{w}_\theta \tag{7}$$

The equation of motion of the fluid is as follows:

$$-\frac{\partial p_f}{\partial r}=\rho_f\ddot{u}_r+\frac{\rho_f}{n}\ddot{w}_r+\frac{1}{K'_d}\dot{w}_r \tag{8}$$

$$-\frac{1}{r}\frac{\partial p_f}{\partial\theta}=\rho_f\ddot{u}_\theta+\frac{\rho_f}{n}\ddot{w}_\theta+\frac{1}{K'_d}\dot{w}_\theta \tag{9}$$

Assuming that the soil particles and fluids are not compressible, the seepage flow equation of continuity in cylindrical coordinates is given as follows:

$$M(\frac{\partial\dot{w}_r}{\partial r}+\frac{\dot{w}_r}{r}+\frac{1}{r}\frac{\partial\dot{w}_\theta}{\partial\theta})+\alpha M(\frac{\partial\dot{u}_r}{\partial r}+\frac{\dot{u}_r}{r}+\frac{1}{r}\frac{\partial\dot{u}_\theta}{\partial\theta})=\dot{p}_f \tag{10}$$

where u_r and u_θ denote the displacement of the soil skeleton along the directions of r and θ, respectively. w_r and w_θ denote the radial and tangential displacement of fluid relative to the soil skeleton. λ and G are the constants of Lame. ρ, ρ_s, and ρ_f are the densities of saturated soil, soil skeleton, and pore water, respectively, where $\rho=(1-n)\rho_s+n\rho_f$. n is the porosity of the soil. p_f is the excess pore water pressure. $k_d'=\dfrac{k_d}{\rho_w g}$, k_d' is the dynamic permeability coefficient of the soil, where k_d is the permeability coefficient of the soil and g is the gravitational acceleration. e is the volume strain of the soil skeleton, where $e=\dfrac{\partial u_r}{\partial r}+\dfrac{u_r}{r}+\dfrac{1}{r}\dfrac{\partial u_\theta}{\partial \theta}+\dfrac{\partial u_z}{\partial z}$. ∇^2 represents the second order operator of Laplace, such that $\nabla^2=\dfrac{\partial^2}{\partial r^2}+\dfrac{1}{r}\dfrac{\partial}{\partial r}+\dfrac{1}{r^2}\dfrac{\partial^2}{\partial \theta^2}+\dfrac{\partial^2}{\partial z^2}$. α and M are the parameters that reflect the compressibility of soil, such that $0\le\alpha\le 1$ and $0\le M\le\infty$, when $M\to\infty$ and $\alpha\to 1$, which means that the particles and pore fluid are not compressible.

Derivations of the equations

The following section introduces the scalar potential function ϕ_1 and ϕ_2, the vector potential function ψ_1 and ψ_2, the displacement vector of the saturated soil skeleton u, and the relative displacement vector of the fluid w:

$$\begin{cases} u_r=\dfrac{\partial\varphi_1}{\partial r}+\dfrac{1}{r}\dfrac{\partial\psi_1}{\partial\theta}, \quad u_\theta=\dfrac{1}{r}\dfrac{\partial\varphi_1}{\partial\theta}-\dfrac{\partial\psi_1}{\partial r} \\ w_r=\dfrac{\partial\varphi_2}{\partial r}+\dfrac{1}{r}\dfrac{\partial\psi_2}{\partial\theta}, \quad w_\theta=\dfrac{1}{r}\dfrac{\partial\varphi_2}{\partial\theta}-\dfrac{\partial\psi_2}{\partial r} \end{cases} \tag{11}$$

By substituting the potential function into Equations. (6) to (10) and separating the vector and scalar, the following equations are obtained:

$$(\lambda+2G+\alpha^2M)\nabla^2\phi_1+\rho\omega^2\phi_1+\alpha M\nabla^2\phi_2+\rho_f\omega^2\phi_2+G\frac{\partial^2\phi_1}{\partial z^2}=0 \tag{12}$$

$$G\nabla^2\psi_1+\rho\omega^2\psi_1+\rho_f\omega^2\psi_2+G\frac{\partial^2\psi_1}{\partial z^2}=0 \tag{13}$$

$$\alpha M\nabla^2\varphi_1+M\nabla^2\varphi_2+\rho_f\omega^2\varphi_1+[\frac{\rho_f}{n}\omega^2-\frac{i\omega}{k_d'}]\varphi_2=0 \tag{14}$$

$$\rho_f\omega^2\psi_1+[\frac{\rho_f}{n}\omega^2-\frac{i\omega}{k_d'}]\psi_2=0 \tag{15}$$

It can be seen that ϕ_1, ϕ_2, ψ_1, and ψ_2 have the same form of the potential function, then

$$\varphi_1=\tilde{\varphi}_1(r,\theta,t)W(z),\ \varphi_2=\tilde{\varphi}_2(r,\theta,t)W(z) \tag{16}$$

$$\psi_1=\tilde{\psi}_1(r,\theta,t)W(z),\ \psi_2=\tilde{\psi}_2(r,\theta,t)W(z) \tag{17}$$

By substituting Equations (16) and (17) into Equations (12) to (15), we arrive at the following equations:

$$\begin{bmatrix} (\lambda+2G+\alpha^2 M)\nabla^2+\rho\omega^2+Gh_1^2 & \alpha M\nabla^2+\rho_f\omega^2 \\ \alpha M\nabla^2+\rho_f\omega^2 & M\nabla^2+[\frac{\rho_f}{n}\omega^2-\frac{i\omega}{k_d{}'}] \end{bmatrix}\begin{bmatrix}\tilde{\varphi}_1\\ \tilde{\varphi}_2\end{bmatrix}=\begin{bmatrix}0\\0\end{bmatrix} \tag{18}$$

$$\begin{bmatrix} G\nabla^2+\rho\omega^2+Gh_2^2 & \rho_f\omega^2 \\ \rho_f\omega^2 & \frac{\rho_f}{n}\omega^2-\frac{i\omega}{k_d'} \end{bmatrix}\begin{bmatrix}\tilde{\psi}_1\\ \tilde{\psi}_2\end{bmatrix}=\begin{bmatrix}0\\0\end{bmatrix} \tag{19}$$

where

$$h_1^2=\frac{1}{W_1}\frac{\partial^2 W_1}{\partial z^2}\,,\ h_2^2=\frac{1}{W_2}\frac{\partial^2 W_2}{\partial z^2} \tag{20}$$

From the boundary conditions of the elastic supporting pile, Equation (3) yields the following:

$$\begin{cases} B_1=B_2;\quad B_3=B_4;\quad h_1=h_2=J_n; \\ \sinh(J_n H)+\frac{k_s}{Gh_n}\cosh(J_n H)=0 \end{cases} \tag{21}$$

where $n=1,2,3,4\cdots\cdots$ defines the horizontal resistance coefficient ratio of the soil $k_s^*=\frac{k_s}{G}$. J_n can be calculated by programming.

To give Equations (18) and (19) an nontrivial solution, the coefficient determinant must be made 0 and then should be simplified as follows:

$$(\nabla^2-\chi_1)(\nabla^2-\chi_2)\tilde{\varphi}_{1,2}=0\,,\ \nabla^2-\chi_3^2=0 \tag{22}$$

where

$$\chi_1+\chi_2=\frac{2\alpha M\rho_f\omega^2-(\lambda+2G+\alpha^2 M)(\frac{\rho_f}{n}\omega^2-\frac{i\omega}{k_d'})}{(\lambda+2G)M}-\frac{\rho\omega^2+GJ_n^2}{\lambda+2G} \tag{23}$$

$$\chi_1\chi_2=\frac{(\rho\omega^2+GJ_n^2)(\frac{\rho_f}{n}\omega^2-\frac{i\omega}{k_d'})-\rho_f^2\omega^4}{(\lambda+2G)M} \tag{24}$$

$$\chi_3^2=-\frac{\rho\omega^2+GJ_n^2}{G}+\frac{\rho_f^2\omega^4}{G(\frac{\rho_f}{n}\omega^2-\frac{i\omega}{k_d'})} \tag{25}$$

Using the operator decomposition theory, $\tilde{\varphi}_{1,2}=\tilde{\varphi}_{1,2}{}^1+\tilde{\varphi}_{1,2}{}^2$, where $\tilde{\varphi}_{1,2}{}^1$ and $\tilde{\varphi}_{1,2}{}^2$ satisfy the following formula:

$$(\nabla^2-\chi_1^2)\tilde{\varphi}_{1,2}{}^1=0\,,\ (\nabla^2-\chi_2^2)\tilde{\varphi}_{1,2}{}^2=0 \tag{26}$$

the solution of Equation (26) is obtained by separation of variables:

$$\tilde{\varphi}_{1,2}{}^{1} = e^{i\omega t}(A^{1}_{1,2}\sin n_1\theta + B^{1}_{1,2}\cos n_1\theta)[C^{1}_{1,2}K_{n_1}(\chi_1 r) + D^{1}_{1,2}I_{n_1}(\chi_1 r)] \tag{27}$$

$$\tilde{\varphi}_{1,2}{}^{2} = e^{i\omega t}(A^{2}_{1,2}\sin n_2\theta + B^{2}_{1,2}\cos n_2\theta)[C^{2}_{1,2}K_{n_2}(\chi_2 r) + D^{2}_{1,2}I_{n_2}(\chi_2 r)] \tag{28}$$

where $K_{n_1}(\chi_1 r)$ and $K_{n_2}(\chi_2 r)$ are the first deformed Bessel function, and $I_{n_1}(\chi_1 r)$ and $I_{n_2}(\chi_2 r)$ are the second. n_1 and n_2 are eigenvalues, and $A^1_{1,2}$, $B^1_{1,2}$, $C^1_{1,2}$, $D^1_{1,2}$, $A^2_{1,2}$, $B^2_{1,2}$, $C^2_{1,2}$, and $D^2_{1,2}$ are undetermined constants. By contacting the boundary conditions in Equation (2), we obtain $D^1_{1,2} = D^2_{1,2} = 0$. From Equation (1), we see that u_r is the even function of θ, and u_θ is the odd function of θ. Then $A^1_{1,2} = A^2_{1,2} = 0$ and $n_1 = n_2 = 1$. Using the finishing coefficient, equations (27) and (28) can be simplified as follows:

$$\varphi_1 = \sum_{n=1}^{\infty} e^{i\omega t}[C_1K_1(\chi_1 r) + C_2K_1(\chi_2 r)]\cos\theta ch(J_n z) \tag{29}$$

$$\varphi_2 = \sum_{n=1}^{\infty} e^{i\omega t}[C_4K_1(\chi_1 r) + C_5K_1(\chi_2 r)]\cos\theta ch(J_n z) \tag{30}$$

$$\psi_1 = \sum_{n=1}^{\infty} e^{i\omega t}C_3K_1(\chi_3 r)\sin\theta ch(J_n z) \tag{31}$$

$$\psi_2 = \sum_{n=1}^{\infty} e^{i\omega t}C_6K_1(\chi_3 r)\sin\theta ch(J_n z) \tag{32}$$

Substituting Equations (29) to (32) into Equations (12) to (15) yields the following:

$$C_4 = c_1C_1,\; C_5 = c_2C_2,\; C_6 = cC_3 \tag{33}$$

where

$$c_1 = -\frac{(\lambda+2G)\chi_1^2 + (\rho-\alpha\rho_f)\omega^2 + GJ_n^2}{\alpha\dfrac{i\omega}{k'_d} + \rho_f\omega^2(1-\dfrac{\alpha}{n})} \tag{34}$$

$$c_2 = -\frac{(\lambda+2G)\chi_2^2 + (\rho-\alpha\rho_f)\omega^2 + GJ_n^2}{\alpha\dfrac{i\omega}{k'_d} + \rho_f\omega^2(1-\dfrac{\alpha}{n})} \tag{35}$$

$$c_3 = \frac{\rho_f\omega^2}{\dfrac{i\omega}{k'_d} - \dfrac{\rho_f}{n}\omega^2} \tag{34}$$

From the stress–strain relationship of saturated soil, the expressions of u_1, u_r, u_θ, w_r, w_θ, σ_r, τ_r can be obtained.

DOI 10.14311/CEJ.2017.02.0010

Decomposing u_1 into a series form results in the following equation:

$$u_1 = \sum_{n=1}^{\infty} U_n ch(J_n z) \quad (37)$$

By contacting the boundary conditions (1) and the impervious conditions of the pile-soil contact surfaces, the following is obtained:

$$\left\{c_1 C_1 [K_1(\chi_1 r)]' + c_2 C_2 [K_1(\chi_2 r)]' + c_3 C_3 K_1(\chi_3 r)/\mathrm{r}\right\}\Big|_{r=r_0} = 0 \quad (38)$$

$$\sum_{n=1}^{\infty} \left\{C_1 [K_1(\chi_1 r)]' + C_2 [K_1(\chi_2 r)]' + C_3 K_1(\chi_3 r)/\mathrm{r}\right\} ch(J_n z)\cos\theta e^{i\omega t}\Big|_{r=r_0} = \sum_{n=1}^{\infty} U_n ch(J_n z)\cos\theta e^{i\omega t} \quad (39)$$

$$\sum_{n=1}^{\infty} \left\{-C_1 K_1(\chi_1 r)/r - C_2 K_1(\chi_2 r)/r - C_3 [K_1(\chi_3 r)]'\right\} ch(J_n z)\sin\theta e^{i\omega t}\Big|_{r=r_0} = -\sum_{n=1}^{\infty} U_n ch(J_n z)\sin\theta e^{i\omega t} \quad (40)$$

3n equations can be got by simultaneous Equations (38) to (40), and simultaneous every three equations corresponding to each n-order mode, the corresponding variables of each equation (C_{1n}, C_{2n} and C_{3n}) can be shown as U_n, and then all coefficients contain only one variable. U_n can be determined from the condition of pile-soil interaction. Below, C_{1n}, C_{2n} and C_{3n} are introduced:

$$C_{1n} = (c_{22}c_{33} - c_{23}c_{32} - c_{12}c_{23} + c_{13}c_{22})/(c_{11}c_{22}c_{33} - c_{11}c_{23}c_{32} - c_{21}c_{12}c_{33} + c_{21}c_{13}c_{32} + c_{31}c_{12}c_{23} - c_{31}c_{13}c_{22})U_n \quad (41)$$

$$C_{2n} = (-c_{21}c_{33} + c_{23}c_{31} + c_{11}c_{23} - c_{13}c_{21})/(c_{11}c_{22}c_{33} - c_{11}c_{23}c_{32} - c_{21}c_{12}c_{33} + c_{21}c_{13}c_{32} + c_{31}c_{12}c_{23} - c_{31}c_{13}c_{22})U_n \quad (42)$$

$$C_{3n} = (c_{21}c_{32} - c_{22}c_{31} - c_{11}c_{22} + c_{12}c_{21})/(c_{11}c_{22}c_{33} - c_{11}c_{23}c_{32} - c_{21}c_{12}c_{33} + c_{21}c_{13}c_{32} + c_{31}c_{12}c_{23} - c_{31}c_{13}c_{22})U_n \quad (43)$$

where $c_{11} = [K_1(\chi_1 r)]'$, $c_{12} = [K_1(\chi_2 r)]'$, $c_{13} = K_1(\chi_3 r)/r$, $c_{21} = c_1[K_1(\chi_1 r)]'$, $c_{22} = c_2[K_1(\chi_2 r)]'$, $c_{23} = c_3 K_1(\chi_3 r)/r$, $c_{31} = -K_1(\chi_1 r)/r$, $c_{32} = -K_1(\chi_2 r)/r$, $c_{33} = -[K_1(\chi_3 r)]'$.

The transverse dynamic reaction force f_{u1} of the pile-side soil to the pile can be calculated. The value of f_{u1} is positive when its direction coincides with the direction of movement. Then, $f_{u1}(z)$ can be represented as follows:

$$f_{u1}(z) = -[\int_0^{2\pi} (\sigma_r \cos\theta - \tau_{r\theta}\sin\theta) r d\theta]\Big|_{r=r_0} \quad (44)$$

$$f_{u1}(z) = -[\int_0^{2\pi} (\sigma_r \cos\theta - \tau_{r\theta}\sin\theta) r d\theta]\Big|_{r=r_0} \quad (44)$$

$$f_{u1}(z) = G\sum_{n=1}^{\infty} ch(J_n z) C_n U_n e^{i\omega t} \quad (45)$$

where $C_n = -\pi r_0[(\lambda + 2G + \alpha M c_1 + \alpha^2 M)B_1 K_1(\chi_1 r_0)\chi_1{}^2 + (\lambda + 2G + \alpha M c_2) + \alpha^2 M)B_2 K_1(\chi_2 r_0 \chi_2{}^2 + G B_3 K_1(\chi_3 r_0)\chi_3{}^2]/G$

SOLVING THE DIFFERENTIAL EQUATION

The differential equation of the single pile under horizontal vibration can be built by considering the dynamic equilibrium conditions when the thickness of thin layer element in the pile is dz.

$$E_pI_p\frac{\partial^4 u_p(z,t)}{\partial z^4}+m_p\frac{\partial^2 u_p(z,t)}{\partial t^2}+G\sum_{n=1}^{\infty}ch(J_nz)C_nU_ne^{i\omega t}=0 \tag{46}$$

where $u_p(z,t)$ is the horizontal displacement of the pile at soil depth of z, E_p and I_p are the elastic moduli and the rotational moment of inertia of the pile, respectively, and m_p is the mass of the pile per unit length.

For steady-state vibration, the horizontal displacement of the pile can be expressed as $u_p(z,t)=U_pe^{i\omega t}$. Substituting this into Equation (46) and simplifying yields, the following equation is obtained:

$$\frac{\partial^4 U}{\partial z^4}-\beta^4U=-\frac{G}{E_pI_p}\sum_{n=1}^{\infty}ch(J_nz)C_nU_ne^{i\omega t} \tag{47}$$

where

$$\beta^4=\frac{m\omega^2}{E_pI_p} \tag{48}$$

For ease of calculation, $e^{i\omega t}$ is omitted. The solution of this fourth order ordinary differential equation is as follows:

$$U_p(z)=f_1\sin(\beta z)+f_2\cos(\beta z)+f_3sh(\beta z)+f_4ch(\beta z)-\sum_{n=1}^{\infty}\frac{GA_n}{E_pI_p(J_n^4-\beta^4)}U_nch(J_nz) \tag{49}$$

According to the contact condition of the pile and soil, the following equation is obtained:

$$f_1\sin(\beta z)+f_2\cos(\beta z)+f_3sh(\beta z)+f_4ch(\beta z)-\sum_{n=1}^{\infty}\frac{GC_n}{E_pI_p(h_n^4-\beta^4)}U_nch(J_nz)=\sum_{n=1}^{\infty}D_nU_nch(J_nz) \tag{50}$$

where

$$D_n=\left\{D_{n1}[K_1(\chi_1r)]'+D_{n2}[K_1(\chi_2r)]'+D_{n3}K_1(\chi_3r)/r\right\}\Big|_{r=r_0} \tag{51}$$

The cosh function $ch(J_nz)$ is an orthogonal function system in $[0,H]$, which means the following:

$$\int_0^H ch(J_nz)ch(J_mz)dz=\begin{cases}L_n, & m=n\\ 0, & m\neq n\end{cases} \tag{52}$$

Multiplying each side of Equation (50) by $ch(J_mz)$ then integrating over $[0,H]$ gives the following:

$$U_n=\frac{M_n}{[\frac{GC_n}{E_pI_p(J_n^4-\beta^4)}+D_n]L_n} \tag{53}$$

where

$$L_n=\int_0^H ch^2(J_nz)=\frac{H}{2}+\frac{ch(J_nH)sh(J_nH)}{2J_n} \tag{54}$$

$$M_{n1}=\int_0^H\ [f_1\sin(\beta z)+f_2\cos(\beta z)+f_3 sh(\beta z)+f_4 ch(\beta z)]ch(J_n z)dz \tag{55}$$

Taking the integral of Equation (3) to (51) gives the following equation:

$$M_{n1}=f_1N_1+f_2N_2+f_3N_3+f_4N_4 \tag{56}$$

where

$$\begin{cases} N_1=[J_n\sin(\beta H)sh(J_nH)-\beta\cos(\beta H)ch(J_nH)+\beta]/(J_n^2+\beta^2) \\ N_2=[J_n\cos(\beta H)sh(J_nH)+\beta\sin(\beta H)ch(J_nH)]/(J_n^2+\beta^2) \\ N_3=[J_n sh(\beta H)sh(J_nH)-\beta ch(\beta H)ch(J_nH)+\beta]/(J_n^2-\beta^2) \\ N_4=[J_n ch(\beta H)sh(J_nH)-\beta sh(\beta H)ch(J_nH)]/(J_n^2-\beta^2) \end{cases} \tag{57}$$

Then U_n can be obtained as follows:

$$\begin{aligned} U_p(z)= {} & f_1[\sin(\beta z)-\sum_{n=1}^{\infty}k_1ch(J_nz)]+f_2[\cos(\beta z)-\sum_{n=1}^{\infty}k_2ch(J_nz)]+f_3[sh(\beta z)-\sum_{n=1}^{\infty}k_3ch(J_nz)] \\ & +f_4[\mathrm{ch}(\beta z)-\sum_{n=1}^{\infty}k_4ch(J_nz)] \end{aligned} \tag{58}$$

where

$$k_1=\vartheta N_1,\ k_2=\vartheta N_2,\ k_3=\vartheta N_3,\ k_4=\vartheta N_4 \tag{59}$$

$$\vartheta=\frac{GC_n}{L_n[E_pI_p(J_n^4-\beta^4)D_n+GC_n]} \tag{60}$$

The rotation amplitude $\theta(z)$, the bending moment amplitude $M(z)$, the displacement amplitude U, and the shear amplitude $Q(z)$ can be obtained using the relations $\theta(z)=U'(z)$, $M(z)=E_pI_pU''(z)$, and $Q(z)=E_pI_pU'''(z)$. By setting the displacement and internal forces of the pile-top for U_0, Φ_0, M_0, and Q_0, and substituting them into Equation (61), the coefficient matrix $[\mathrm{T(z)}]$ can be calculated.

$$\begin{pmatrix} U_p \\ \theta \\ M/(E_pI_p) \\ Q/(E_pI_p) \end{pmatrix}=\begin{bmatrix} t_{11}(z) & t_{12}(z) & t_{13}(z) & t_{14}(z) \\ t_{21}(z) & t_{22}(z) & t_{23}(z) & t_{24}(z) \\ t_{31}(z) & t_{32}(z) & t_{33}(z) & t_{34}(z) \\ t_{41}(z) & t_{42}(z) & t_{43}(z) & t_{44}(z) \end{bmatrix}\begin{pmatrix} f_1 \\ f_2 \\ f_3 \\ f_4 \end{pmatrix}=[T(z)]\begin{pmatrix} f_1 \\ f_2 \\ f_3 \\ f_4 \end{pmatrix} \tag{61}$$

f_{11_1}, f_{21_1}, f_{31_1}, and f_{41_1} are coefficients if it is assumed that unit horizontal displacement occurs in the pile-top, which can be solved by the boundary condition:

$$\begin{cases} z=0: U_{p1}(0)=1,\theta_{p1}(0)=0 \\ z=l_1: \dfrac{\partial^3U_{p1}(l_1)}{\partial z^3}+k_{p1}^*U_{p1}(l_1)=0, M_{p1}(l_1)=0 \end{cases} \tag{62}$$

The impedance in the pile-tip can be calculated as follows:

$$\begin{aligned} K_{h1} &= f_{11\_1}t_{41}(0)+f_{21\_1}t_{42}(0)+f_{31\_1}t_{43}(0)+f_{41\_1}t_{44}(0) \\ &= F_{h1}+iF_{h2} \end{aligned} \tag{63}$$

$$\begin{aligned} K_{rh1} &= f_{11\_1}t_{31}(0)+f_{21\_1}t_{32}(0)+f_{31\_1}t_{33}(0)+f_{41\_1}t_{34}(0) \\ &= F_{rh1}+iF_{rh2} \end{aligned} \tag{64}$$

f_{11_2}, f_{21_2}, f_{31_2}, and f_{41_2} are coefficients when unit horizontal displacement occurs in the pile-top, and can be also solved by a boundary condition as follows:

$$\begin{cases} z=0: U_{p1}(0)=0,\ \theta_{p1}(0)=1 \\ z=l_1: \dfrac{\partial^3 U_{p1}(l_1)}{\partial z^3}+k_{p1}^{*}U_{p1}(l_1)=0,\ M_{p1}(l_1)=0 \end{cases} \tag{65}$$

The impedance in the pile-tip can be calculated using the following equation:

$$\begin{aligned} K_{hr1} &= f_{11\_2}t_{41}(0)+f_{21\_2}t_{42}(0)+f_{31\_2}t_{43}(0)+f_{41\_2}t_{44}(0) \\ &= F_{hr1}+iF_{hr2} \end{aligned} \tag{66}$$

$$\begin{aligned} K_{r1} &= f_{11\_2}t_{31}(0)+f_{21\_2}t_{32}(0)+f_{31\_2}t_{33}(0)+f_{41\_2}t_{34}(0) \\ &= F_{r1}+iF_{r2} \end{aligned} \tag{67}$$

Equations (62), (63), (66), and (67) are impedances in the pile-top. For ease of calculation, the dynamic factors of an elastic supporting pile under horizontal vibration can be defined as follows: $f_{r1}=\dfrac{F_{r1}}{E_pI_p}$, $f_{r2}=\dfrac{F_{r2}}{E_pI_p}$, $f_{h1}=\dfrac{F_{h1}}{E_pI_p}$, $f_{h2}=\dfrac{F_{h2}}{E_pI_p}$, $f_{rh1}=\dfrac{F_{rh1}}{E_pI_p}$, $f_{rh2}=\dfrac{F_{rh2}}{E_pI_p}$, $f_{hr1}=\dfrac{F_{hr1}}{E_pI_p}$, $f_{hr2}=\dfrac{F_{hr2}}{E_pI_p}$.

MODEL VALIDATION

To validate the rationality of the theory in this paper, the lateral complex impedance factors were used as a sample, with $k_p^*=10$, $H/r_0=10$, $k_d'=10^{-6}$, $E_p=25.5GPa$, $\rho_p=2500kg/m^3$, $\rho_s=2700kg/m^3$, $\rho_f=1000kg/m^3$, $\alpha=1$, $n=0.375$, $G=10MPa$, and $v=0.25$. Contrastive analysis was explored to calculate the lateral complex impedance in the pile-tip using an elastic supporting pile and a rigid supporting pile. Custom frequency ratio $a_0=\omega/\omega_g$, ω and ω_g are vibration frequency and first order primary frequency of soil ($\omega_g=\dfrac{V_s}{2H}(2n-1)\pi, n=1,2,3...$).

Figure 2 shows that when the horizontal stiffness coefficient of the pile bottom is reasonable, the model described in this paper produces similar results to the model of a rigid supporting pile. This means that if the stiffness in the tip of an elastic supporting pile is large enough, it is reasonable to simplify it as a rigid supporting pile.

DOI 10.14311/CEJ.2017.02.0010

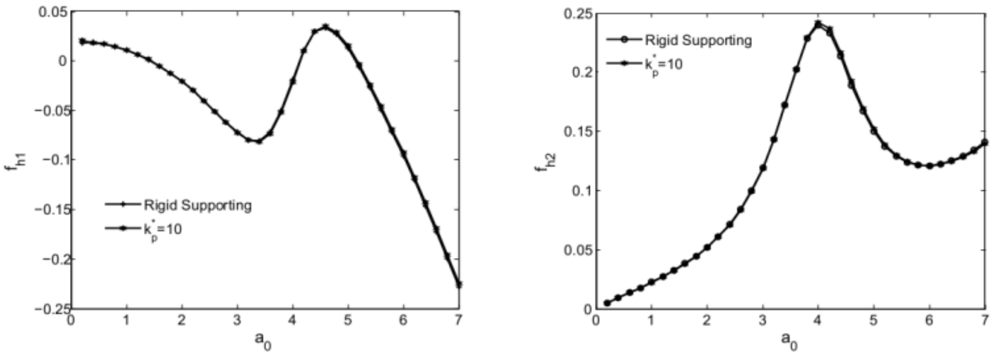

Fig. 2 - Comparison of present model (in this work) and the model of a rigid supporting pile

HORIZONTAL DYNAMIC PARAMETRIC ANALYSIS OF THE ELASTIC SUPPORTING PILE

To analyse the influence of the lateral elastic anti-displacement coefficient of the soil k_s and the lateral elastic anti-displacement coefficient in the pile-tip k_p, the lateral complex impedance factors were used samples.

Influence of the lateral resistance coefficient of the pile-tip on lateral complex impedance of the pile-top

The relationship curve between the lateral resistance coefficient of the pile-tip on the lateral complex impedance and the frequency of the pile-top is shown in Figure 3, when $H/r_0 = 10, 20, 40$, $k_p^* = 0, 0.01, 0.1, 1, 10, 1000$. The horizontal resistance coefficient ratio in the pile-top k_p^* reflects the bearing capacity of the pile-bottom medium to pile-tip. The greater is its value, the stronger is the ability of the pile-tip to resist horizontal displacement and the larger is the horizontal displacement stiffness of the pile bottom. When k_p^* is infinite, the elastic supporting pile can be equivalent to a rigid supporting pile.

Figure 3 depicts that the horizontal complex stiffness factor in the pile-tip appears to have more obvious peaks and troughs. The smaller is the horizontal resistance coefficient in the pile-tip, the larger is the wave amplitude of the horizontal complex stiffness in the pile-top and the more obvious is the influence of the horizontal resistance coefficient ratio in the pile-tip.

When the ratio of the length to diameter is small, the changes of k_p^* have a large impact on the complex stiffness in the pile-tip and will generate large fluctuations in the horizontal, swing, or horizontal-swing complex impedance amplitude. With an increase in the ratio of length to diameter, the horizontal resistance in the pile-tip becomes less obvious, and the volatility in the corresponding vibration frequency grows. This means that the complex impedance in a pile-tip with a small ratio of length to diameter is more susceptible to the influence of the horizontal resistance coefficient in the pile bottom.

For the pile of larger diameter, when the frequency is low (especially the low-frequency range relevant to power foundation design), the horizontal resistance coefficient in the pile-tip has almost no effect on the horizontal complex impedance in the pile-top. As the frequency increases, the influence of the lateral resistance coefficient of the pile-tip on lateral complex impedance of the pile-top increases.

DOI 10.14311/CEJ.2017.02.0010

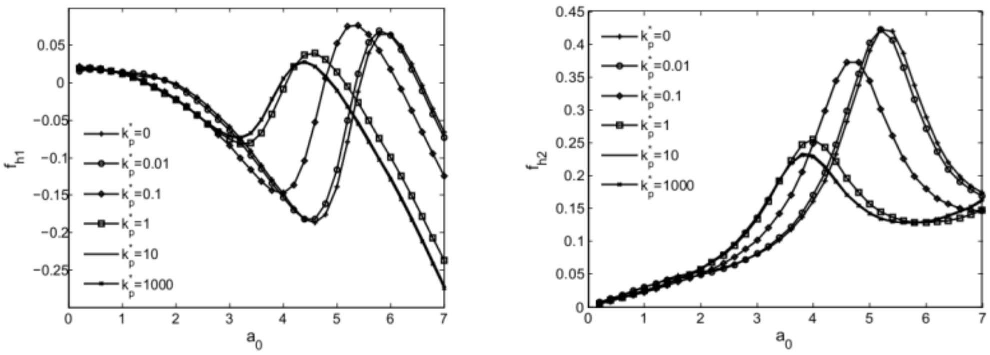

(a) $H / r_0 = 10$

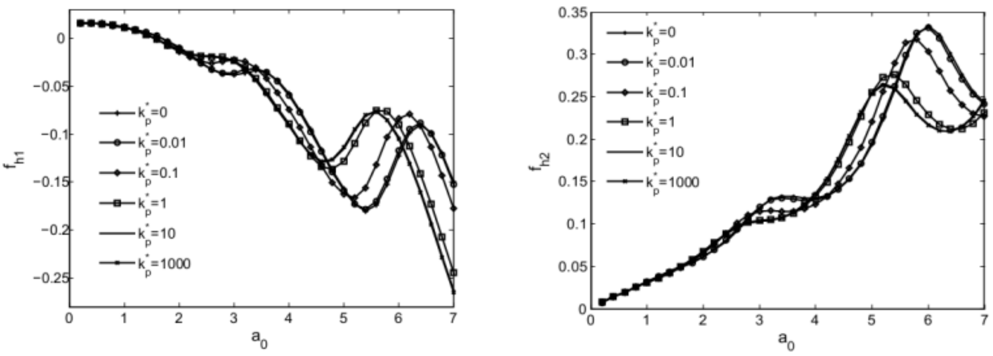

(b) $H / r_0 = 20$

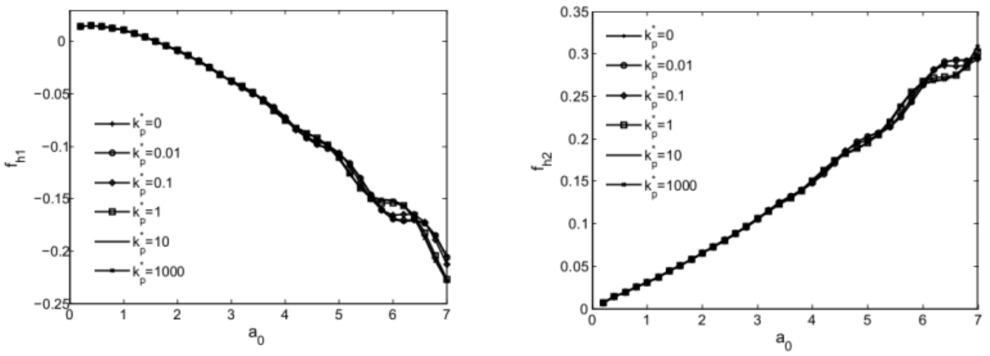

(c) $H / r_0 = 40$

Fig. 3 - Influence of lateral resistance coefficient ratio of the pile-tip on lateral complex impedance factors in the pile-top

Influence of lateral resistance coefficient of soil on the lateral complex impedance of the pile-top

Figure 4 depicts the relationship curve when the lateral resistance coefficient ratio of soil is $k_p^* = 0, 0.01, 0.1, 1, 10, 1000$. Under the conditions of low frequency (with vibration frequency smaller than 0.35 *Hz*) and soft soil around the pile lateral, the changes of the horizontal resistance coefficient in the pile bottom exert great influence on the impedance function and amplitude frequency in the pile-top.

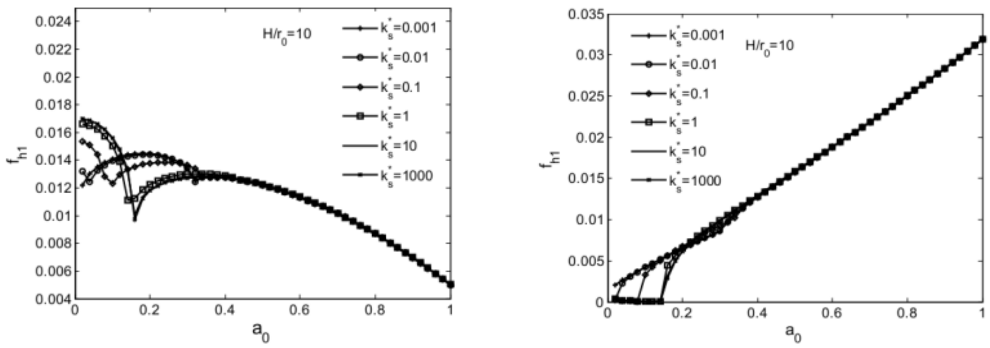

(a) $H / r_0 = 10$

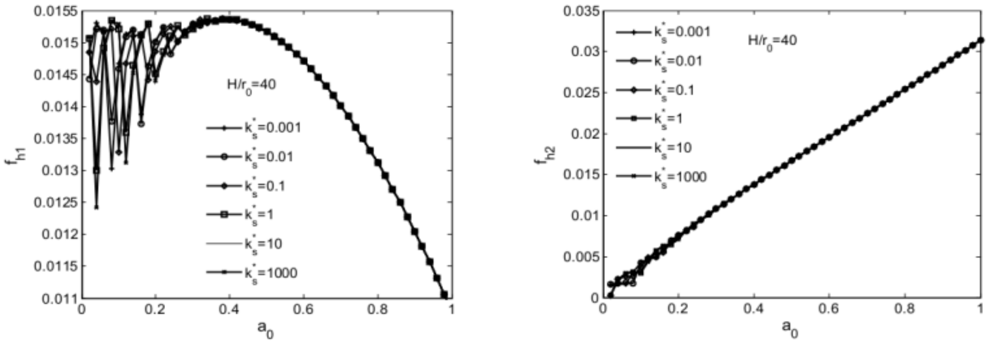

(b) $H / r_0 = 40$

Fig. 4 - Influence of the lateral resistance coefficient ratio of soil on the lateral complex impedance of the pile-top

In the physical mechanism, under the conditions of low frequency and soft soil, wave propagation follows the horizontal direction. The horizontal connection condition of the pile-tip (horizontal reaction coefficient of soil around the pile bottom) has an influence on the complex impedance factor in the pile-top. Under conditions of high frequency (the vibration frequency is greater than 0.35 Hz) this effect is not obvious.

The characteristics of the complex stiffness factor in the pile-top were studied under conditions of low frequency, small length-diameter ratio, and soft soil around the pile lateral. The amplitude of resonance in the piles and soil is small and fluctuates quite gently. When the ratio of length to diameter is larger, the resonance amplitude of the pile is bigger and the wave is more obvious. Boundaries as the elastic modulus of soil under pile, when the force coefficient is larger than the elastic modulus, the force coefficient in the pile bottom will no longer have an impact on the impedance in the pile-top

CONCLUSION

This work derived the analytical solution of an elastic supporting pile embedded in saturated soil under horizontal vibration. We substantiated the validity of this method by retrogressed verification of the model, and analyzed the influence of elastic support for lateral complex impedance in a pile-top.

ACKNOWLEDGEMENTS

This work was supported by the National Science & Technology Pillar Program during the Twelfth Five-year Plan Period (2012BAB03B02).

REFERENCES

[1] Novak M, 1974. Dynamic stiffness and damping of piles. Canadian Geotechnical Journal, vol. 11: 574-598. DOI: 10.1139/T74-059.

[2] Nogami T, Novak M, 1977. Resistance of soil to a horizontally vibrating pile. Earthquake Engineering and Structural Dynamics, vol. 5: 249-261. DOI: 10.1002/eqe.4290050304.

[3] Novak M, Aboul-Ella F, 1978. Impedance functions of piles in layered media. Journal of the Engineering Mechanics Division, vol. 104: 643-661.

[4] Zheng CJ, Liu HL, Ding XM, 2016. Lateral dynamic response of a pipe pile in saturated soil layer. International Journal for Numerical and Analytical Methods in Geomechanics, vol. 40: 159-184. DOI: 10.1002/nag.2388.

[5] Yang J, Song EX, Chen ZY, 2002. Simple radiation damping model for horizontally vibration pile in saturated soil. Rock and Soil Mechanics, vol. 23: 179-183. DOI: 10.16285/j.rsm.2002.02.011. (in Chinese)

[6] Shang SP, Yu J, Wang HD, Ren H, 2007. Horizontal vibration of piles in saturated soil. Chinese Journal of Geotechnical Engineering, vol. 29: 1696-1702. DOI: 10.3321/j.issn:1000-4548.2007.11.017 (in Chinese)

[7] Liu HL, Zheng CJ, Ding XM, Qin HY, 2014. Vertical dynamic response of a pipe pile in saturated soil layer. Computers and Geotechnics, vol. 61: 57-66. DOI: 10.1016/j.compgeo.2014.04.006.

[8] Yu J, Shang SP, Zhong L, Ren H, 2009. Study of resitance factor of saturated soil caused by horizontal vibration of pile. Rock and Soil Mechanics, vol. 30: 3858-3864. DOI: 10.16285/j.rsm.2009.12.051. (in Chinese)

[9] Ding XM, Liu HL, Liu JY, Chen YM, 2011. Wave Propagation in a Pipe Pile for Low-Strain Integrity Testing. Journal of Engineering Mechanics, vol. 137: 598-609. DOI: 10.1061/(ASCE)EM.1943-7889.0000263.

[10] Chow YK, Phoon KK, Chow WF, Wong KY, 2003. Low strain integrity testing of piles: Three-dimensional effects. Journal of Geotechnical and Geoenvironmental Engineering, vol. 129(11): 1057-1062. DOI: 10.1061/(ASCE)1090-0241.

[11] Xu X.T., Liu H.L., Lehane B.M., 2006. Pipe pile installation effects in soft clay. Proceedings of the Institution of Civil Engineers - Geotechnical Engineering, vol. 159: 285-296. DOI: 10.1680/geng.2006.159.4.285

[12] Liu HL, Chu J, Deng A, 2009. Use of large-diameter cast-in situ concrete pipe piles for embankment over soft clay. Canadian Geotechnical Journal, vol. 46: 915-927. DOI: 10.1139/T09-032.

[13] Zienkiewicz OC, Chan AHC, Pastor M, Shiomi T, 1987. Computational Approach to Soil Dynamics. Developments in Geotechnical Engineering, vol. 26: 1169-1184. DOI: 10.1016/B978-0-444-98958-1.50005-4.